Int. J. Heat Mass Transfer. Vol. 29, No. 12, pp. 1881–1889, 1986
Printed in Great Britain

0017–9310/86 $3.00 + 0.00
Pergamon Journals Ltd.

Laminar flow with an axially varying heat transfer coefficient

BRIAN VICK and R. G. WELLS

Mechanical Engineering Department, Virginia Polytechnic Institute and State University, Blacksburg, VA 24061, U.S.A.

(*Received* 21 *October* 1985 *and in final form* 13 *March* 1986)

Abstract—A theoretical study of convective heat transfer in laminar duct flow subjected to an axial variation of the external heat transfer coefficient is presented. Since standard analytical techniques are not applicable, a variable eigenvalue approach is developed which is capable of handling variable boundary condition parameters. Methodology is presented for the case of a stepwise periodic variation of the heat transfer coefficient, which serves as a model for a duct fitted with an array of external fins. A parameter study showing the effects of a stepwise periodic heat transfer coefficient is presented which gives insight into heat transfer enhancement due to finning.

INTRODUCTION

HEAT transfer to forced flow in conduits has been the subject of numerous investigations, leading all the way back to the original Graetz problem [1]. Various geometries and thermal boundary conditions, such as specified temperature, specified heat flux, or convection with an external environment via a constant heat transfer coefficient, have been extensively investigated. An excellent review of the works performed up to 1978 is presented by Shah and London [2]. Despite this wealth of literature, there appears to be no analytical solution available for a fluid exchanging heat with an external environment whose heat transfer coefficient varies along the axial direction. The reason that such a problem, with many important applications, remains unresolved is that the conventional techniques, such as Green's functions or finite integral transform, all fail when applied to problems involving a variable boundary condition parameter. Thus, the objective of the present investigation is to develop the solution methodology capable of handling forced convection with a varying external heat transfer coefficient. The solution will be utilized in performing a systematic parameter study for the case of fully developed, laminar flow in a tube.

There are many applications for a thermal boundary condition which varies along the flow direction. One example is heat transfer enhancement due to external fins. Since a fin increases the effective coefficient of heat exchange between the fin base and the ambient, a duct fitted with an array of external fins can be modeled as an unfinned duct with a periodically low and high value of the heat transfer coefficient, corresponding to unfinned and finned regions, respectively. This model was used by Sparrow and Charmchi [3] to examine heat transfer from an externally finned, circular tube using a finite-difference scheme; however, the periodic stepwise nature of the thermal boundary condition made the computational task quite demanding, and a complete parameter study was not feasible.

Potential applications for enhancement of heat transfer by the use of extended surfaces are plentiful. Finned ducts are encountered, for example, in residential or industrial space heating. Also condensers, evaporators and other heat exchange equipment are often augmented by the use of fins. Laminar flow applications for enhanced heat transfer include heating or cooling of viscous liquids in the chemical and food industries, heating or cooling of oils, heating of the circulating fluid in solar collectors, heat transfer in compact heat exchangers, and the cooling or warming of blood during surgical operations. While existing systems can often be improved by using an augmented method, the design of heat exchangers for use in space vehicles, aircraft or nuclear reactors require mandatory heat transfer enhancement in order for the system to function properly and meet the size and weight limitations imposed.

The present investigation is intended to give insight into the heat transfer characteristics associated with these applications. In a more general sense, the investigation is intended to shed light on solution methodology for problems involving variable boundary condition parameters.

MATHEMATICAL MODEL

The present investigation focuses on the thermal entry region in a conduit with steady, fully developed flow entering at temperature T_0, as shown schematically in Fig. 1. The duct has convective boundaries exchanging heat with an environment at temperature T_∞ by virtue of an axially varying heat transfer coefficient, $h(z)$. The governing energy equation

NOMENCLATURE

a_{mp}	coefficients defined by equation (14b)	$\bar{u}$	average velocity
$A_{mp}(\xi)$	coefficients defined by equation (10b)	$v(\eta)$	dimensionless velocity
$\mathbf{A}_k$	matrix defined by equation (16b)	z	axial variable.
$g(r,z)$	energy source		
$h(z)$	heat transfer coefficient	Greek symbols	
$H(\xi)$	Biot number	α	thermal diffusivity
k	thermal conductivity	Γ_m^+	transforms after a jump point
Pe	Péclet number	Γ_m^-	transforms before a jump point
$Q(\xi)$	total heat transfer	η	dimensionless radial variable
r	radial variable	$\theta(\eta,\xi)$	dimensionless temperature
$S(\eta,\xi)$	dimensionless energy source	$\theta_b(\xi)$	bulk temperature
$\bar{S}_m(\xi)$	transformed energy source	$\bar{\theta}_m(\xi)$	transformed temperature
$T(r,z)$	temperature	$\lambda_m(\xi)$	variable eigenvalue
T_∞	environment temperature	ξ	dimensionless axial variable
T_0	inlet temperature	$\psi_m(\eta,\xi)$	variable eigenfunction
$u(r)$	velocity profile	μ	viscosity.

and boundary conditions, in dimensionless form, are taken as

$$\frac{v(\eta)}{2}\frac{\partial\theta}{\partial\xi}=\frac{1}{\eta^i}\frac{\partial}{\partial\eta}\left(\eta^i\frac{\partial\theta}{\partial\eta}\right)+S(\eta,\xi),$$

$$0<\eta<1,\quad \xi>0 \tag{1a}$$

$$\frac{\partial\theta}{\partial\eta}=0,\quad \eta=0 \tag{1b}$$

$$\frac{\partial\theta}{\partial\eta}+H(\xi)\theta=0,\quad \eta=1 \tag{1c}$$

$$\theta=1,\quad \xi=0. \tag{1d}$$

The various dimensionless quantities are defined as

$$\eta=r/r_0,\quad \xi=\frac{z/r_0}{Pe} \tag{2a}$$

$$Pe=\frac{2r_0\bar{u}}{\alpha},\quad v(\eta)=\frac{u(r)}{\bar{u}} \tag{2b}$$

$$\theta(\eta,\xi)=\frac{T(r,z)-T_\infty}{T_0-T_\infty} \tag{2c}$$

$$H(\xi)=\frac{h(z)r_0}{k} \tag{2d}$$

$$S(\eta,\xi)=\frac{[g(r,z)+\mu(\partial u/\partial r)^2]r_0^2}{k(T_0-T_\infty)}. \tag{2e}$$

Energy equation (1a) includes a choice of both geometry, through the exponent i, and velocity profile, through the function $u(r)$, as follows

$$i=\begin{cases}0, & \text{parallel plates}\\ 1, & \text{circular tube}\end{cases} \tag{3}$$

$$u(r)=\begin{cases}\bar{u}, & \text{slug flow}\\ \frac{3}{2}\bar{u}\left[1-\left(\frac{r}{r_0}\right)^2\right], & \text{fully developed flow, parallel plates}\\ 2\bar{u}\left[1-\left(\frac{r}{r_0}\right)^2\right], & \text{fully developed flow, circular tube.}\end{cases} \tag{4}$$

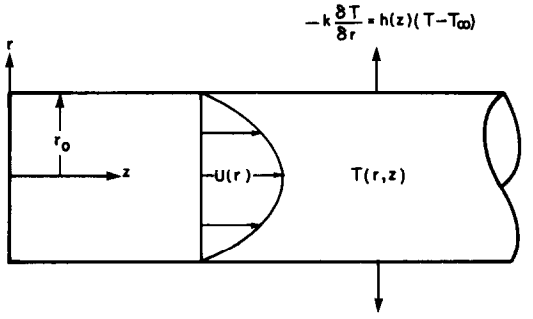

FIG. 1. Geometry and coordinates.

Other velocity profiles may also be selected for applications such as the flow of a non-Newtonian fluid. The dimensionless source term, $S(\eta,\xi)$, includes both the effects of viscous energy dissipation and thermal energy generation, as seen from definition (2e). Also, axial diffusion has been omitted and the fluid properties have been taken as constant.

Many special cases of engineering interest can be obtained from the system of equations (1) by merely specifying the functional form of the heat transfer coefficient, $H(\xi)$. However, this flexibility in modeling is accompanied by mathematical difficulties when an analytical solution is attempted. Although the prob-

lem given by the system of equations (1) is relatively easy to describe and is solvable when $H(\xi)$ is constant [4], solutions for a variable Biot number become surprisingly difficult since the nonseparable nature of the problem causes conventional analytical procedures to fail.

In the following section, we develop a generalized finite integral transform technique which is capable of handling such problems involving variable boundary condition parameters. The technique allows for accurate computations and for a complete study of the system parameters.

GENERAL ANALYSIS

In order to solve the problem of interest, as described by the system of equations (1), we adopt a variable eigenfunction technique which was originally applied to transient heat conduction by Özişik and Murray [5]. The technique is based on the following variable eigenvalue problem

$$\frac{\partial}{\partial\eta}\left(\eta^i\frac{\partial\psi_m}{\partial\eta}\right)+\lambda_m^2(\xi)\eta^i\frac{v(\eta)}{2}\psi_m(\eta,\xi)=0 \tag{5a}$$

$$\frac{\partial\psi_m}{\partial\eta}=0,\quad \eta=0 \tag{5b}$$

$$\frac{\partial\psi_m}{\partial\eta}+H(\xi)\psi_m=0,\quad \eta=1. \tag{5c}$$

Here the axial variable ξ is treated as a parameter. At any given axial location the Biot number, $H(\xi)$, has some definite value and we have a corresponding set of eigenfunctions, $\psi_m(\eta,\xi)$, and eigenvalues, $\lambda_m(\xi)$. These eigenfunctions obey the following normalized orthogonality relation

$$\int_{\eta=0}^{1}\eta^i\frac{v(\eta)}{2}\psi_m(\eta,\xi)\psi_p(\eta,\xi)\,d\eta=\begin{cases}0, & m\neq p\\ 1, & m=p.\end{cases} \tag{6}$$

At any given axial location, the eigenfunctions form a complete set and the temperature field, $\theta(\eta,\xi)$ can subsequently be constructed from an infinite series of these functions. Using orthogonality relation (6), we can develop in the usual manner the following transform pair

Transform:

$$\bar{\theta}_m(\xi)=\int_{\eta=0}^{1}\eta^i\frac{v(\eta)}{2}\psi_m(\eta,\xi)\theta(\eta,\xi)\,d\eta \tag{7a}$$

Inversion:

$$\theta(\eta,\xi)=\sum_{m=1}^{\infty}\psi_m(\eta,\xi)\bar{\theta}_m(\xi). \tag{7b}$$

We now find the transforms by operating on energy equation (1a) with

$$\int_{\eta=0}^{1}\eta^i\psi_m(\eta,\xi)\,d\eta.$$

After utilizing boundary conditions (1b,c) and (5b,c), we arrive at the following expression

$$\int_{\eta=0}^{1}\eta^i\frac{v(\eta)}{2}\psi_m(\eta,\xi)\frac{\partial\theta}{\partial\xi}d\eta=-\lambda_m^2(\xi)\bar{\theta}_m(\xi)+\bar{S}_m(\xi) \tag{8}$$

where

$$\bar{S}_m(\xi)=\int_{\eta=0}^{1}\eta^i\psi_m(\eta,\xi)S(\eta,\xi)\,d\eta. \tag{9}$$

Since our eigenfunctions, $\psi_m(\eta,\xi)$, depend on ξ, the partial derivative cannot be brought outside the integral on the LHS of expression (8). Instead, we resort to the eventual form of our solution given by the inversion formula, equation (7b). After substituting equation (7b) for $\theta(\eta,\xi)$ in equation (8) and manipulating, we obtain the following result

$$\frac{d\bar{\theta}_m}{d\xi}+\lambda_m^2(\xi)\bar{\theta}_m+\sum_{p=1}^{\infty}\bar{\theta}_p(\xi)A_{mp}(\xi)=\bar{S}_m(\xi),$$
$$m=1,2,3,\ldots,\quad \xi>0 \tag{10a}$$

where the variable coefficients have been defined as

$$A_{mp}(\xi)=\int_{\eta=0}^{1}\eta^i\frac{v(\eta)}{2}\psi_m(\eta,\xi)\frac{\partial\psi_p}{\partial\xi}d\eta. \tag{10b}$$

The initial conditions are obtained by taking the transform of equation (1d) to get

$$\bar{\theta}_m=\frac{H(0)\psi_m(1,0)}{\lambda_m^2(0)}=B_m,\quad m=1,2,3,\ldots,\quad \xi=0. \tag{10c}$$

The system of equations (10) constitutes an infinite set of coupled, first-order ordinary differential equations with variable coefficients for the transforms, $\bar{\theta}_m(\xi)$. The key to getting numerically accurate results lies in the successful solution of this set for the desired variation of the dimensionless heat transfer coefficient, $H(\xi)$. The following section describes the solution procedure for the computationally demanding case where $H(\xi)$ varies in a stepwise periodic manner.

TRANSFORMS FOR STEPWISE PERIODIC CASE

The system of equations (10) governing the transforms are quite sensitive to the axial variation of the coefficients, $A_{mp}(\xi)$, and eigenvalues, $\lambda_m(\xi)$, which in turn depend on the variation of the Biot number, $H(\xi)$. If $H(\xi)$ varies in a continuous manner in the flow direction, the corresponding functional forms of $A_{mp}(\xi)$ and $\lambda_m(\xi)$ will also be continuous, resulting in continuity of the transforms. However, a computationally more difficult case involves a stepwise periodic Biot number, as depicted in Fig. 2. This case has particular interest since it could serve as a model for a duct fitted with an array of external fins, with

unfinned and finned regions corresponding to low and high Biot numbers, respectively [3].

The function shown in Fig. 2 may be expressed as

$$H(\xi) = \begin{cases} H_1, & \xi^*_{1j} < \xi < \xi^*_{2j} \\ H_2, & \xi^*_{2j} < \xi < \xi^*_{1,j+1} \end{cases} \quad (11a)$$

where $j = 0, 1, 2, \ldots$.

For convenience we have designated the jump points by

$$\begin{aligned} \xi^*_{1j} &= j(\xi_1 + \xi_2) \\ \xi^*_{2j} &= j(\xi_1 + \xi_2) + \xi_1. \end{aligned} \quad (11b)$$

Eigenvalue problem (5) also follows this stepwise behavior and we designate the solutions as

$$\lambda_m(\xi) = \begin{cases} \lambda_{1m}, & \xi^*_{1j} < \xi < \xi^*_{2j} \\ \lambda_{2m}, & \xi^*_{2j} < \xi < \xi^*_{1,j+1} \end{cases} \quad (12a)$$

$$\psi_m(\eta, \xi) = \begin{cases} \psi_{1m}(\eta), & \xi^*_{1j} < \xi < \xi^*_{2j} \\ \psi_{2m}(\eta), & \xi^*_{2j} < \xi < \xi^*_{1,j+1} \end{cases}. \quad (12b)$$

The nature of the transforms resulting from the system of equations (10) will also involve discontinuities at each jump point. Recognizing this discontinuous nature, we adopt the following notation for the transforms on either side of a jump point

$$\Gamma^-_m(\xi^*_{kj}) = \lim_{\varepsilon \to 0} \bar{\theta}_m(\xi^*_{kj} - \varepsilon) \quad (13a)$$

$$\Gamma^+_m(\xi^*_{kj}) = \lim_{\varepsilon \to 0} \bar{\theta}_m(\xi^*_{kj} + \varepsilon) \quad (13b)$$

where $k = 1$ or 2, $j = 0, 1, 2, \ldots$.

Turning to the coefficient functions, we evaluate definition (10b) by observing the stepwise nature of the eigenfunction as expressed in equation (12b). The variation of $\partial\psi_p/\partial\xi$ is seen to be a delta function at each jump point and zero everywhere else while the eigenfunction assumes an average value at each point of discontinuity. Thus equation (10b) can be evaluated as

$$A_{mp}(\xi) = a_{mp} \sum_{j=0}^{\infty} [\delta(\xi - \xi^*_{2j}) - \delta(\xi - \xi^*_{1,j+1})] \quad (14a)$$

where

$$a_{mp} = \frac{H_2 - H_1}{2} \left[\frac{\psi_{1m}(1)\psi_{2p}(1)}{\lambda^2_{2p} - \lambda^2_{1m}} - \frac{\psi_{2m}(1)\psi_{1p}(1)}{\lambda^2_{2m} - \lambda^2_{1p}} \right]. \quad (14b)$$

Equation (14a) shows that the coefficients, $A_{mp}(\xi)$, give no contribution to the system of equations (10a) except at each jump point, where they contribute an impulse, or a delta function.

With this behavior in mind, we may formally integrate equation (10a) from the beginning of a constant Biot number region, $\xi = \xi^*_{kj}$, up to an arbitrary location before the next jump point. The result is simply

$$\bar{\theta}_m(\xi) = \Gamma^+_m(\xi^*_{kj}) \exp[-\lambda^2_{km}(\xi - \xi^*_{kj})] + \int_{\xi' = \xi^*_{kj}}^{\xi} \exp[-\lambda^2_{km}(\xi - \xi')] \bar{S}_m(\xi')\, d\xi' \quad (15)$$

which is valid for

$$\xi^*_{1j} < \xi < \xi^*_{2j} \quad \text{when } k = 1$$

$$\xi^*_{2j} < \xi < \xi^*_{1,j+1} \quad \text{when } k = 2$$

where $j = 0, 1, 2, \ldots$ and $m = 1, 2, 3, \ldots$.

We now have reduced the problem to finding the values $\Gamma^+_m(\xi^*_{kj})$. We thus integrate equation (10a) from $\xi = \xi^*_{kj} - \varepsilon$ to $\xi = \xi^*_{kj} + \varepsilon$ and take the limit as $\varepsilon \to 0$. After carefully observing the discontinuous nature of $\bar{\theta}_m(\xi)$, the delta function contribution of the $A_{mp}(\xi)$ functions, and the continuous behavior of the necessary integrating factor, we may express the result of this integration in matrix form as

$$\mathbf{A}_k \boldsymbol{\Gamma}^+(\xi^*_{kj}) = \boldsymbol{\Gamma}^-(\xi^*_{kj}) \quad (16a)$$

where

$$\mathbf{A}_k = \begin{bmatrix} 2 & (-1)^k a_{12} & (-1)^k a_{13} & \cdots \\ (-1)^k a_{21} & 2 & (-1)^k a_{23} & \cdots \\ \vdots & & & \end{bmatrix} \quad (16b)$$

$$\boldsymbol{\Gamma}^+(\xi^*_{kj}) = \begin{bmatrix} \Gamma^+_1(\xi^*_{kj}) \\ \Gamma^+_2(\xi^*_{kj}) \\ \vdots \end{bmatrix} \quad (16c)$$

$$\boldsymbol{\Gamma}^-(\xi^*_{kj}) = \begin{bmatrix} 2\Gamma^-_1(\xi^*_{kj}) - (-1)^k \sum_{p=1}^{\infty} a_{1p}\Gamma^-_p(\xi^*_{kj}) \\ 2\Gamma^-_2(\xi^*_{kj}) - (-1)^k \sum_{p=1}^{\infty} a_{2p}\Gamma^-_p(\xi^*_{kj}) \\ \vdots \end{bmatrix} \forall \quad (16d)$$

The solution for a stepwise periodic Biot number is now complete since equation (15) gives expressions for the transforms with the $\Gamma^+_m(\xi^*_{kj})$ values obtained from the solution of matrix equation (16a), truncated at a finite number of terms. Since the solution in any given region depends on the previous region, computations proceed from the duct entrance and continue downstream, with the $\Gamma^+_m(\xi^*_{kj})$ values required for each region. Numerical results using this solution will now be used to demonstrate the technique and the heat transfer characteristics of flow subjected to a variable boundary condition coefficient.

RESULTS AND DISCUSSIONS

Heat transfer results for the stepwise periodic Biot number depicted in Fig. 2 are now presented. Viscous energy dissipation and internal heat sources are neglected by setting $S(\eta, \xi) = 0$ in energy equation (1a). Most of the results are presented for fully

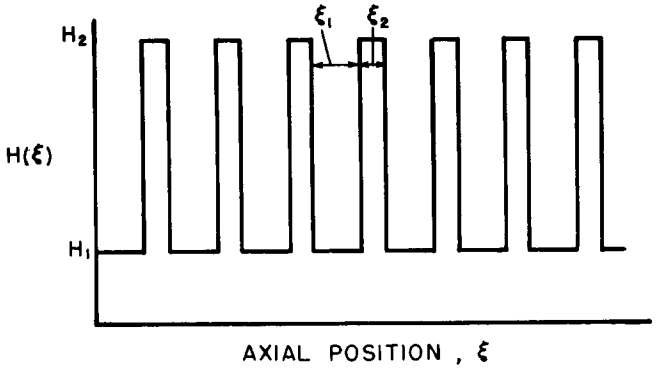

FIG. 2. Stepwise periodic Biot number.

developed laminar flow in a tube ($i = 1$, $u(r) = 2\bar{u}[1-(r/r_0)^2]$) since this case has the greatest practical interest and since the accuracy of the analytical technique can be compared directly with the finite-difference results of ref. [3]. Other possible cases include slug flow in parallel plates or circular tubes and fully developed laminar flow in parallel plates. The only difference among all these cases is the specific functions generated from eigenvalue problem (5), where slug flow in parallel plates gives trigonometric functions, slug flow in circular tubes gives Bessel functions, and fully developed laminar flow in parallel plates and tubes necessitates the use of Graetz functions [6]. Although the numerical results would differ somewhat, the essential features and heat transfer characteristics for all these cases are similar.

Graphical results are presented for the total heat transfer, which in the absence of energy sources and viscous dissipation is given by the quantity

$$Q(\xi) = 1-\theta_b(\xi). \tag{17}$$

The bulk temperature is defined as

$$\theta_b(\xi) = \int_{\eta=0}^{1} (2\eta)^i v(\eta)\theta(\eta,\xi)\,d\eta. \tag{18}$$

Using inversion formula (7b) and eigenvalue problem (5), equation (18) can be evaluated as

$$\theta_b(\xi) = 2^{i+1}H(\xi)\sum_{m=1}^{\infty}\frac{\psi_m(1,\xi)}{\lambda_m^2(\xi)}\bar{\theta}_m(\xi). \tag{19}$$

The dimensionless quantity $Q(\xi)$ given by equation (17) represents the total energy transferred from the fluid up to some axial location ξ, divided by the total energy transferred as a condition of thermal saturation is reached at sufficiently large ξ. Regardless of the axial variation or magnitude of the Biot number, $H(\xi)$, a state of thermal saturation will eventually be reached where the fluid temperature approaches the external environment temperature. The only exception is the uninteresting case of $H(\xi) = 0$, for which the fluid remains at the inlet temperature. Since the periodic stepwise Biot number serves as a model for a duct fitted with an array of external fins, the quantity $Q(\xi)$ is a meaningful way to display the advantages of heat transfer enhancement due to finning.

The transforms, $\bar{\theta}_m(\xi)$, required in equation (19) are available for the stepwise periodic case from equation (15) with $\bar{S}_m(\xi) = 0$. The values $\Gamma_m^+(\xi_{kj}^*)$ are obtained from matrix equation (16a). The number of terms required for convergence in series solution (19) depends mainly on $\xi-\xi_{kj}^*$, which is the axial distance from the previous point where the Biot number changed. For a typical value of $\xi-\xi_{kj}^* = 0.001$, approximately 10 terms are required for convergence to three significant figures. In order to obtain comparable accuracy for the $\Gamma_m^+(\xi_{kj}^*)$ values, matrix equation (16a) was solved for 100 elements. As a check on the accuracy of the present method, numerical results were obtained for several cases with constant Biot number ($H_1 = H_2$) and these results were found to be indistinguishable from other exact methods [2]. For the much more demanding case of $H_1 \neq H_2$, the only available comparison is with the finite-difference solution of Sparrow and Charmchi [3]. Here again the results using the present analytical solution were indistinguishable from the numerical solutions presented in ref. [3].

Turning our attention to Fig. 3, we see the total heat transfer, $Q(\xi)$, plotted as a function of axial distance ξ. For a finned duct, the length ξ_1 represents the interfin spacing while ξ_2 represents the fin thickness. The low Biot number represents the external heat transfer coefficient for unfinned areas while H_2 represents the effective Biot number in finned areas.

Figure 3 displays results for a constant Biot number along with the effect of heat transfer enhancement due to larger values of H_2. The results are identical for all cases until the first Biot number jump is encountered at $\xi = 0.003$. At this point the effect of the enhanced heat exchange causes the total heat transfer to rise sharply, with a larger H_2 giving a steeper rise. The enhancement is most significant in the entrance region, with the effects diminishing downstream as all curves approach thermal saturation.

The discontinuous variation of the external heat transfer coefficient causes the step-like nature shown in Fig. 3. For convenience, the details of these steps

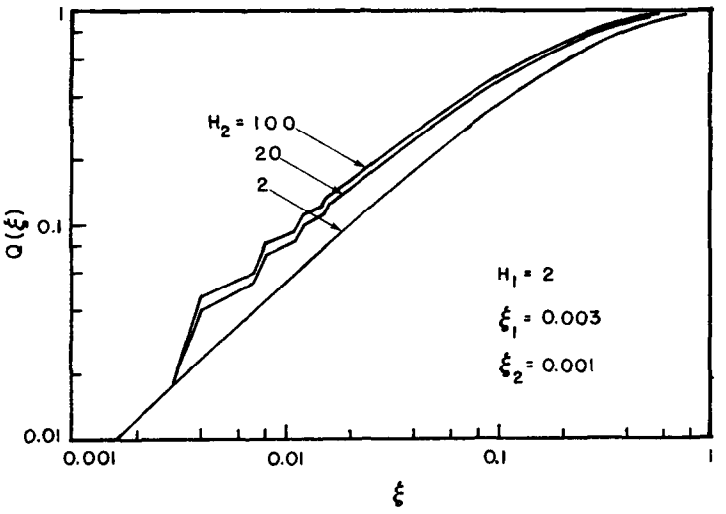

FIG. 3. Effect of H_2 on total heat transfer.

have been plotted in only the first few regions. The total heat transfer rises at a high rate in regions of large Biot number and rises at a smaller rate in regions of diminished Biot number. This step-like behavior makes purely numerical schemes quite demanding [3] and is the reason that standard analytical techniques fail when applied to present problems.

We put these results in perspective with the help of Fig. 4. Here we display the same results as in Fig. 3 except that all values of the Biot number have been divided by a factor of 2. Although the results of Figs. 3 and 4 are qualitatively similar, we see that the effect of enhanced heat transfer is more pronounced when the overall level of the Biot number is decreased, particularly in the thermal entry region. To investigate this further, we present Fig. 5 where the Biot number ratio is fixed at $H_2/H_1 = 20$ while the overall level changes. At the relatively low level with $H_1 = 1$, enhancement has a significant effect as the slope of the total heat transfer curve takes sharp turns whenever a region of different H is encountered. This is in contrast to the results for $H_1 = 20$, where the overall level is already so high that enhancing the heat transfer has a much smaller effect. This is because the internal resistance to heat flow is the controlling factor once the external resistance becomes quite low.

We now examine the effect of interfin spacing in Fig. 6. Here we show results for $\xi_1 = 0.001, 0.005$ and ∞, while holding ξ_2, H_1 and H_2 constant. The case where $\xi_1 \to \infty$ is equivalent to the constant Biot number case of $H = H_1 = 1$. Figure 6 shows that the smaller values of ξ_1 give the greatest enhancement since the proportion of duct without fins is reduced. Again the effects are most pronounced in the duct entrance with all curves approaching thermal saturation further downstream.

Additional insight into geometric effects is gained from Fig. 7. Here the ratio ξ_1/ξ_2 remains fixed at 3

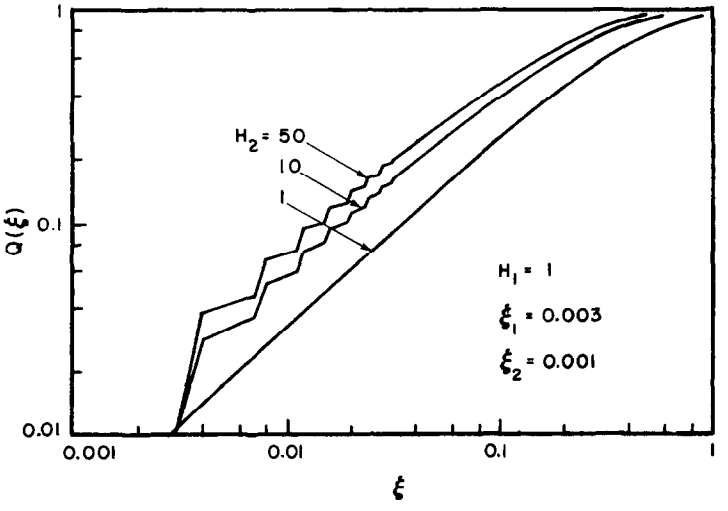

FIG. 4. Effect of H_2 on total heat transfer.

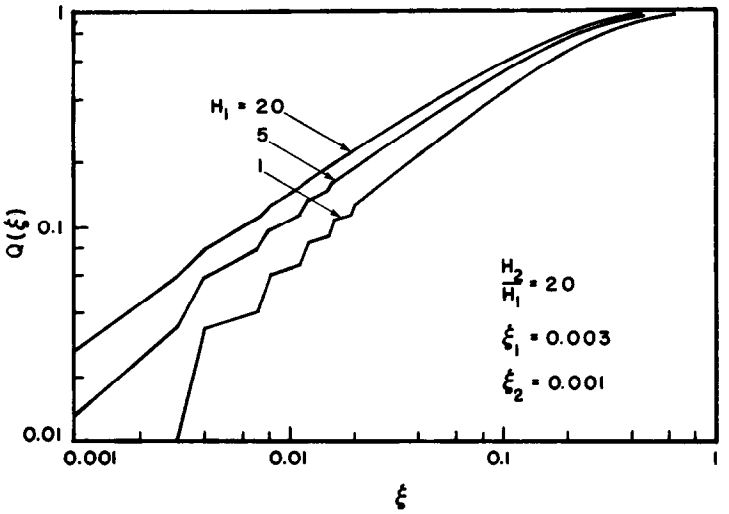

FIG. 5. Effect of the overall Biot number level on total heat transfer.

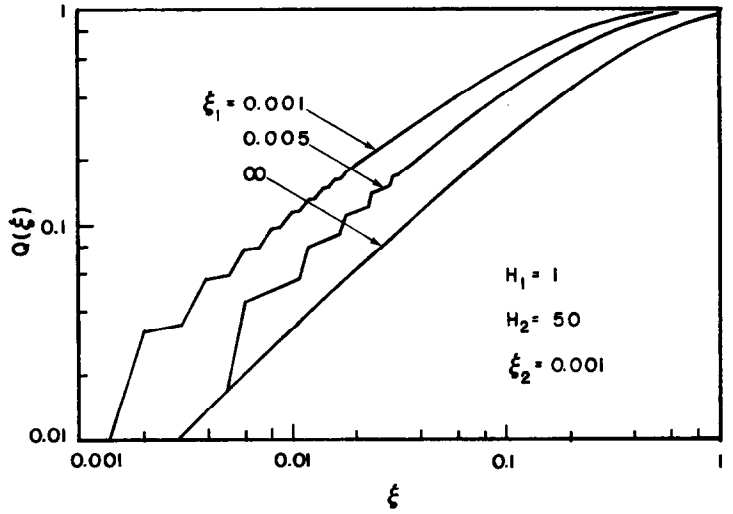

FIG. 6. Effect of ξ_1 (interfin spacing) on total heat transfer.

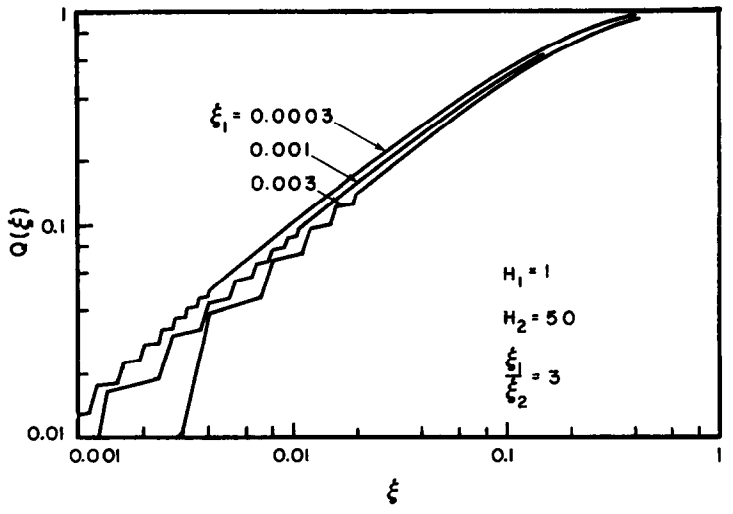

FIG. 7. Effect of cycle frequency on total heat transfer.

while the frequency of low and high Biot number cycles is changed. The case where $\xi_1 = 0.003$ represents a relatively large spacing or low frequency. The curves for $\xi_1 = 0.001$ and 0.0003 show very little increase in heat transfer once the first region of high Biot number or first fin is encountered. This means that we can increase the frequency of fins by 3 or even 10 times and gain a relatively small increase in total heat transfer, as long as the ratio ξ_1/ξ_2 remains constant. The more effective means to increase heat transfer is to make the ratio ξ_1/ξ_2 smaller, as seen in Fig. 6.

The influence of the assumed velocity profile is examined in Fig. 8, where the effect of heat transfer enhancement resulting from the parameter H_2 is presented for both laminar and slug flow. Note that the step-like nature displayed in previous graphs has been smoothed by passing a curve through the midpoint of each region. This process is illustrated in the laminar flow curve for $H_2 = 20$, where a portion of the step-like behavior is also displayed. As seen in Fig. 8, the total heat transfer is greater at any given axial location for slug flow than for laminar flow. This is due to the greater velocity in the wall region for slug flow which effectively lowers the internal thermal resistance. With a lower internal resistance, greater heat transfer can be achieved for any given level of the external resistance. The slug flow results are expected to be characteristic of turbulent flow results, since turbulence enhances both the momentum and energy transport processes and thus lowers the internal thermal resistance.

CONCLUSIONS

The present investigation concerns forced convection in laminar duct flow subject to an axial variation of the external heat transfer coefficient or Biot number. Although the governing equations are relatively easy to describe and seem quite harmless, they are surprisingly difficult to solve. Since the variable heat transfer coefficient makes the problem non-separable, all standard analytical procedures fail and a variable eigenvalue approach is developed which is capable of handling variable boundary condition parameters. Methodology is developed to handle a stepwise periodic Biot number since this case serves as a model for a duct fitted with an array of regularly spaced fins and also represents the most computationally demanding test for the general analysis.

A parameter study is presented which displays the effects of heat transfer enhancement due to finning for laminar flow in a tube. It is demonstrated that the total heat transfer can be increased significantly by enhancing the effective heat transfer coefficient using fins. Augmentation is the most beneficial when the overall level of the external Biot number is low, since the external thermal resistance is high. Heat transfer is also sensitive to the proportion of duct with fins, while the frequency of the fins has relatively little influence. The effect of velocity profile is also examined. Due to a higher velocity and a lower internal resistance near the wall, the slug flow gives greater heat transfer than the laminar flow.

Although numerical results are provided for a stepwise periodic Biot number and are related to the application of a finned tube, the general analysis can be applied to any variation of the external Biot number which can be used to model a variety of situations. For instance, the effects of axial conduction in the tube wall could be included by specifying a harmonic or smoothed out variation of the Biot number. Also, a variety of other applications can be readily modeled including periodically contacting surfaces, thermal quenching, transient heat conduction with time varying heat transfer coefficient and phase change problems. The methodology presented should lend insight into the solution for this general class of problems involving variable boundary condition parameters.

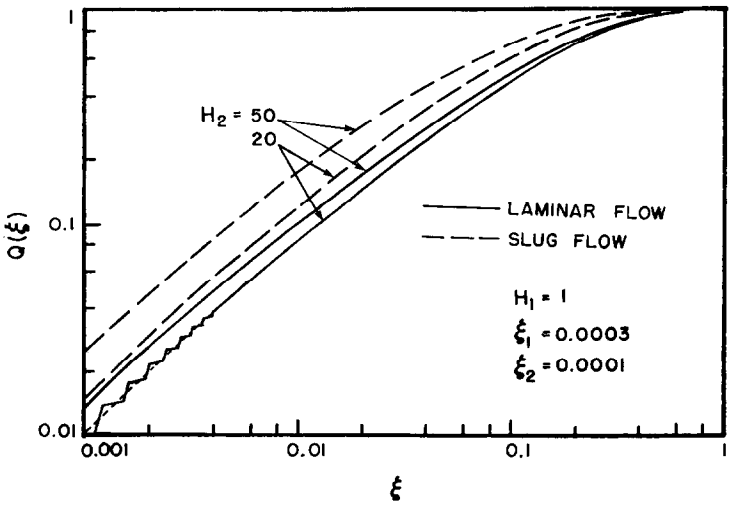

FIG. 8. Effect of velocity profile on total heat transfer.

Acknowledgement—This work was supported by the National Science Foundation through Grant No. MEA-8403964.

REFERENCES

1. L. Graetz, Uber die Wärmeleitungsfähigheit von Flüssigkeiten, *Annln Phys. Chem.* **25,** 337–357 (1885).
2. R. K. Shah and A. L. London, *Laminar Flow Forced Convection in Ducts.* Academic Press, New York (1978).
3. E. M. Sparrow and M. Charmchi, Laminar heat transfer in an externally finned circular tube, *J. Heat Transfer* **102,** 605–611 (1980).
4. V. Javeri, Heat transfer in laminar entrance region of a flat channel for the temperature boundary condition of the third kind, *Warme- u. Stoffubertr.* **10,** 137–144 (1977).
5. M. N. Özişik and R. L. Murray, On the solution of linear diffusion problems with variable boundary condition parameters, *J. Heat Transfer* **96,** 48–51 (1974).
6. J. R. Sellars, M. Tribus and J. S. Klein, Heat transfer to laminar flow in a round tube or flat conduit—the Graetz problem extended, *Trans. Am. Soc. mech. Engrs* **78,** 441–447 (1956).

ECOULEMENT LAMINAIRE AVEC UN COEFFICIENT DE CONVECTION THERMIQUE VARIABLE SUIVANT L'AXE

Résumé—On présente une étude théorique de convection thermique pour un écoulement laminaire dans un tube soumis à une variation axiale du coefficient de transfert thermique. Puisque les techniques analytiques standard ne sont pas applicables, on développe une approche par valeurs propres qui est capable de traiter des paramètres de condition limite variable. La méthodologie est présentée dans le cas d'une variation périodique en créneaux du coefficient de transfert thermique qui modélise un canal équipé d'ailettes externes. Une étude paramétrique sur les effets d'un coefficient de transfert périodique en créneaux permet de comprendre l'accroissement du transfert thermique dû aux ailettes.

LAMINARE STRÖMUNG MIT EINEM AXIAL SICH ÄNDERNDEN WÄRMEÜBERGANGSKOEFFIZIENTEN

Zusammenfassung—Es wird eine theoretische Studie des konvektiven Wärmeübergangskoeffizienten in einer laminaren Kanalströmung abhängig von einem in axialer Richtung sich ändernden äußeren Wärmeübergangskoeffizienten gezeigt. Da die allgemein üblichen analytischen Methoden hier nicht anwendbar sind, wurde eine variable Eigenwertmethode entwickelt, welche die Anwendung von variablen Randbedingungen ermöglicht. Das Verfahren wird für das Beispiel eines sich schrittweise periodisch ändernden Wärmeübergangskoeffizienten gezeigt, welches als Modell für einen außen berippten Kanal dient. Eine Parameterstudie zeigt den Einfluß eines schrittweise periodischen Wärmeübergangskoeffizienten und gibt einen Einblick in die Erhöhung des Wärmeübertragungsvermögens durch eine Berippung.

ЛАМИНАРНОЕ ТЕЧЕНИЕ С ПЕРЕМЕННЫМ ВДОЛЬ ОСИ КОЭФФИЦИЕНТОМ ТЕПЛОПЕРЕДАЧИ

Аннотация—Теоретически изучается конвективный теплоперенос при ламинарном течении в канале с продольно изменяющимся коэффициентом теплопередачи. Поскольку известные методы к данному случаю не применимы, развит подход переменных собственных значений для переменных граничных условий. Рассмотрен случай ступенчатого периодического изменения коэффициента теплопередачи, которая является моделью для канала с внешним оребрением. Представлен параметрический анализ влияния ступенчатого периодического изменения коэффициента теплообмена, который объясняет усиление теплопереноса за счет оребрения.